Thermal Performance of Film Cooling for Two Staggered Rows of Circular Jet

Dr. Assim H. Yousif
Machines & Equipments Engineering Department, University of Technology/Baghdad
Dr. Amer M. Al-Dabagh
Machines & Equipments Engineering Department, University of Technology/Baghdad
Dr. Muwafag Sh. Alwan
Electromechanical Engineering Department, University of Technology/Baghdad
Email:abulaithmsh@yahoo.com

Received on: 13/12/2011 & Accepted on: 7/6/2012

ABSTRACT

The holes orientation and jet inclination angles are important parameters that control the development of the flow structures and the penetration and spreading of the jets. Experimental investigations that describe the film cooling performance for a two rows of staggered holes with opposite orientation angles are presented to determine the heat transfer coefficient and film effectiveness under different holes attitude. Experimentalin vestigations were done on a flat plate by using a single test transient IR thermograph technique. The attitude of the downstream row holes is fixed at inclination angle (θ=30°) and orientation angle of (γ=0°), while the upstream row holes is fixed with opposite orientation angle (γ=180°) and the inclination angles are changed three times as (θ=20°, 30°, and40°). Three different blowing ratios (BR) =0.5, 1.0, and 1.5 are used in experimental program at each case. Enhancements were observed, in which as theblowing ratio increased and the inclination angle of upstream row decreased, the film cooling effectiveness and heat transfer coefficient are increased.

الأداء الحراري لغشاء التبريد لصفين من النفاثات الدائرية المتعرجة

الخلاصة

أن زوايا الأتجاه والميل لثقوب النفث من المعالم المهمة المؤثره على بنية وتداخل وأنتشار النفاثات. لحساب معامل أنتقال الحراره وفعالية غشاء التبريد، تم أجراء تجارب عمليه لصفين من الفتحات المتعرجه الترتيب لزوايا أتجاه وميل مختلفه ولنسب نفخ متنوعه. وقد تم أجراء التجارب بأستخدام تقنية الصوره الحراريه دون الحمراء(IR) على صفيحه مستويه بألية الفحص الأنتقالي الواحد.حيث تم تثبيت زاوية الميل بمقدار 30º وزاوية الأتجاه بمقدار 0º بالنسبه للصف النازل(downstream) ، بينما تم تثبيت زاوية الأتجاه للثقوب في صف الصاعد(upstream) بمقدار 180º وتغيير زاوية الميلان ثلاث مرات هي:20º, 30º, 40º ،ولكل حاله من الحالات تم أستخدام ثلاث قيملنسب النفخ وهي .(BR=0.5, 1.0, 1.5). أظهرت النتائج أن تقليل زاوية الميل للثقوب في الصف الصاعد وزيادة نسب النفخ أدت الى زيادة فعالية غشاء التبريد ومعامل أنتقال الحراره.

https://doi.org/10.30684/etj.2013.71249
2412-0758/University of Technology-Iraq, Baghdad, Iraq

Nomenclatures

BR blowing ratio
D film hole diameter
h heat transfer coefficient with coolant injection**.**
h_o heat transfer coefficient without coolant injection**.**
k thermal conductivity of test surface.
q heat flux with coolant injection.
q_o heat flux without coolant injection.
t time when the IR image was captured.
T_c coolant air temperature.
T_f film temperature.
T_i initial temperature.
T_m mainstream temperature.
T_w prescribed wall temperature.
U_c coolant air velocity.
U_m mainstream air velocity.
η film effectiveness.
η_{sa} spanwise average film cooling effectiveness.
η_o average film cooling effectiveness.
Ø overall cooling effectiveness.
$\propto$ thermal diffusivity.
γ orientation angle.
θ inclination angle.
θ_{us} inclination angle of upstream holes row.
A_o selected area.

INTRODUCTION

Modern gas turbine engines are designed to perform at high inlet temperature of (1800-2000 ºK) to improve thermal efficiency and power output. As the turbine inlet temperature increases, the heat transferred to the blades in the turbine also increases. Since this temperature exceeds the melting point of the turbine blade materials of about (≈ 1480 K). Therefore, there is a need for an efficient cooling system engineered in away such that the maximum blade surface temperature during operation is well below the maximum melting point of the blade material. To achieve that, researchers focus on various innovative cooling techniques depending on the nature of the coolant flow.

Film cooling primarily depends on the coolant-to-mainstream pressure ratio or can be related to the blowing ratio, temperature ratio (T_c/T_m), and the film cooling hole location, configuration and distribution on a turbine elements film cooling. In atypical gas turbine blade, the range of the blowing ratios are of about approximately between 0.5 and 2.0, while the (Tc/Tm) values vary between 0.5 and 0.85 **Han andEkkad[1].**

Han and Rallabandi[2] stated that the pressure sensitive paint technique proved very high resolution contours of film cooling effectiveness, without being subjected to the conduction error in high thermal gradient regions near the hole.**Ahn et al. [3]** presented the injectant behavior from two rows of film cooling

holes with opposite orientation angles. Four film cooling hole arrangements were considered including inline and staggered ones. Detailed adiabatic film cooling effectiveness distributions were also measured using Thermochromic Liquid Crystal (TLC) to investigate how well the injectant covers the film cooled surface.Later.

Maitehand Jubran [4] presented experimental investigation the effect of pressure gradient on the film cooling effectiveness for five models, each consisted of two rows of holes. Both rows having compound angle holes or both rows having simple angle holes or combination of one row of simple angle holes and the other row of compound angle holes. Results showed that the presence of a favorable pressure gradient tends to increase the dilution of the injected coolant jet, which results in a reduction of the film cooling protection over the surface. The presence of an adverse pressure gradient at high blowing rate tends to dilute the film coolant even at a higher rate than that when zero or Favorable pressure gradient are present.**Dhungel et al. [5]**obtained simultaneously detailed heat transfer coefficient and film effectiveness measurements using a single test transient IR thermography technique for a row of cylindrical film cooling holes, shaped holes. A number of anti-vortex film cooling designs that incorporate side holes. They found that the presence of anti-vortex holes mitigates the effect of the pair of anti-vortices.

Also**Lu et al. [6 and7]** presented the experimental and numerical investigation of film cooling performance for a row of cylindrical holes in modern turbine blade. The adiabatic film effectiveness and heat transfer coefficient are determined experimentally on a flat plate downstream of a row of inclined different geometries hole exit by using a single test transient IR thermograph techniqueat four different coolant-to-mainstream blowing ratios of 0.5, 1.0, 1.5 and 2.0. Four test designs crescent and converging slot, trench and cratered hole exits, are tested. Results showed that both the crescent and slot exits reduce the jet momentum at exit and also provide significantly higher film effectiveness with some increases in heat transfer coefficients.

Diaand Lin [8] investigated numerically three film cooling configurations, (cylindrical hole, shaped hole, crescent hole). All holes were inclined at 35° on a flat plate. All simulations are conducted at blowing ratio of 0.6 and 1.25, length to diameter ratio of 4 and pitch-t0-diameter ratio of 3. They use (RANS) equations, the energy equation, and two-layer $(k-\epsilon)$ turbulence models. For the numerical investigation the commercial CFD software FLUENT with standard $(k-\epsilon)$ turbulent models is applied. They found that the crescent hole exhibits the highest film cooling effectiveness among the three configurations both in spanwise and streamwise especially downstream of the interaction of the two holes.

Lee and Kim [9] evaluatedthe effect of geometric variables of a laidback fan-shaped hole on the film cooling effectiveness using a Reynolds-averaged Navier-stokes analysis. The shape of the laidback fan-shaped hole is defined by four geometric design variables: the injection angle of the hole, the lateral expansion angle of the diffuser, the forward expansion angle of the hole, and the ratio of the length to diameter of the hole. They concluded that the increase of the forward expansion angle makes a reduction of film cooling effectiveness, and the lateral

expansion angle has the biggest impact among the four geometric variables on the spatially averaged film cooling effectiveness.

At the present work, experimentalinvestigations were done to evaluate thefilm effectiveness and heat transfer coefficient on a flat plate by using a single test transient IR thermograph techniquefor a two rows of staggered jet holes of opposite orientation angles and at different blowing ratio and jet inclination angles.

EXPERIMENTAL FACILITIES

Low speed open duct jet test rigwas designed and manufactured to be used at the present investigation. A schematic diagram and photograph of the test rigare shown in figures(1) and (2). The mainstream air supply is the ambient air drawn by a centrifugal backward blade blower. The blower is driven by 2.5 kW motor running with 2800 rpm. Manual open gate is used to control the air speed in the tunnel test section.The blower exit area having rectangular shape with dimensions of (6.3x13.1) cm. The blower is supplied with bend having the same dimensions of the blower exist and then connected to a diffuser having rectangular cross-section area of inlet and outlet dimensions as (6.3x13.1) cm and (35x50) cm respectively and length of (82) cm. Air flow diffuses over a splitter plates into a constant area rectangular settling chamber of cross-section area (35x50) cm and length of 70 cm. The settling chamber contains a series of three electrical heaters each of 4 kW power and four grid screen. This ensures adequate mixing of hot air and uniform temperature distribution throughout the test section. Then the hot air routed through a convergent- divergent contraction having a rectangular cross-section area from (35x50) cm to (5x10) cm and length of 70 cm. In order to allow the air to reach the desired temperature, the air is initially routed out away from the test section by using a by-bass gate passage. The temperature of the air is continuously monitored at the exit of the gate and when the desired temperature is reached, the gate is fully opened manually and air flow passes into a test section through a rectangular duct area. To minimize heat losses to the surrounding the settling chamber and the test section duct are insulated completely. The operating velocity of the hot air in the test section is controlled to run from 20 to 40m/s through the experimental program.The test section has 50mm width and 100mm height. The bottom plate of the test section is made of (234x123) mm Plexiglas of 10mm thickness.

A centrifugal air blower of blowing capacity of (22.17) m^3/min was used to supply the coolant air to the plenum. The plenum was located below the test plate. The coolant air enters a plenum then ejected through holes into the test section. The coolant air pressure measured at the inlet of the test section. Digital thermometers were used to measure the mainstream and coolant airtemperature. Pre-testing showed that all holes had the same flow rate and temperature conditions. Finally the flow from the coolant holes and the mainstream combine in the test section as shown in figure (1).

Two rows of staggered holes with opposite orientation angles are included in the present study.The orientation angles (θ) is defined as the hole orientation toward the cross-flow in the mainstream andthe inclination angle(θ)is defined as the angle between the centerline of the hole and the surface of the test wall. Figure (3) shows the rows arrangements. For the downstream row holes, the orientation angles and the inclination angle are fixed at(θ= 0°) and (θ=30°) respectively, while

atthe upstream row ϒ is fixed at180°and the inclination angle of upstream holes row (θ_{us}) are changedas cas1 (θ_{us}=20º), cas2 (θ_{us}= 30º), and cas3 (θ_{us}= 40º).

Thearrangement of holes geometry were taken as, the hole diameter (D=4mm), the longitudinal distance between the rows (X) is four time (D), and the span distance between each neighboring holes (Z) is three time (D).

The surface temperature of test plate was measured using an infrared thermographs technique. Single test transient IR thermograph technique is used as infrared camera type Fluke Ti32. This camera was able to precisely record temperature variations. The IR system is greatly affected by both background temperature and local emissivity. The test surface is sprayed with mat black color to increase the emissivity like a perfect black body. The temperature measurement taken is not accurately recorded unless the IR system is calibrated.

The system is calibrated by measured the temperature of the test surface using thermocouple type Kfixed in test surface, in same time the temperature is measured by the IR camera. The test surface is heated by hot mainstream. The temperatures obtained by both measuring way is recorded during the heating process until achieving a steady state condition. Due to the emissivity of the test surface the temperature recorded by IR camera is differed from the temperature obtained by the thermocouple, and then IR camera is adjusted until both reading temperatures are matched.

The IR images taken for the test surfaces at each test are stored in the SD memory of IR camera. These images are transferred from SD memory to PC memory. Then the middle region of the test surface area is then selected to eliminate the effect of the test section wall with using camera software, Smart View Software Program. IR images, which exhibit the temperatures distribution as colors code, is converted to corresponding temperature digit values by using Smart View Software and then saved as output data in Excel sheet.

PROCEDURE

Consider the transient flow over a flat plate as shown in figure (4). In this case, the test plate is initially at a uniform temperature T_i, and the convective boundary condition is suddenly applied on the plate at time t >0. Now, heat assumed to be conducted only in the x-direction and perform an energy balance on the plate, therefore the one-dimensional transient conduction equation is

$$\frac{\partial^2 T}{\partial x^2} = \frac{1}{\propto} \frac{\partial T}{\partial t} \qquad \text{...(1)}$$

The main approximation often applied to analyze transient conduction shown in Figure (5) is the semi-infinite approximation. The semi-infinite solid assumptions are valid for our case for two reasons. The test duration is small, usually less than 60 seconds. Secondly, the hot air flowing over the test surface made from Plexiglas of, low thermal conductivity, low thermal diffusivity, and low lateral conduction. The solution of equation (1) is given by [10] as the follow.

$$\frac{T_w - T_i}{T_m - T_i} = 1 - exp\left(\frac{h^2 \propto t}{k^2}\right) erfc\left(\frac{h\sqrt{\propto t}}{k}\right) \qquad \text{...(2)}$$

Where T_w is measured by using IR camera, all the other variables in the equation (2) are either known or measured except the heat transfer coefficient (h).

In film cooling case, the film should be treated as a mixture of air mainstream and the coolant air, as shown in figure 5, the mainstream temperature (T_m) in equation(2) has to be replaced by the film temperature (T_f), therefore equation (2) become as:

$$\frac{T_w - T_i}{T_f - T_i} = 1 - exp\left(\frac{h^2 \propto t}{k^2}\right) erfc\left(\frac{h\sqrt{\propto t}}{k}\right) \quad \dots \quad (3)$$

A non-dimensional temperature term is known as the film cooling effectiveness (η), and is defined as:

$$\eta = \frac{T_f - T_m}{T_c - T_m} \quad \dots \quad (4)$$

Equation (3) has two unknowns, (h and T_f), to solve this equation, two sets of data points required to obtain the unknowns like:

$$\frac{T_{w1} - T_i}{T_f - T_i} = 1 - exp\left(\frac{h^2 \propto t1}{k^2}\right) erfc\left(\frac{h\sqrt{\propto t1}}{k}\right) \quad \dots \quad (5)$$

$$\frac{T_{w2} - T_i}{T_f - T_i} = 1 - exp\left(\frac{h^2 \propto t2}{k^2}\right) erfc\left(\frac{h\sqrt{\propto t2}}{k}\right) \quad \dots \quad (6)$$

In this case, a transient infrared thermograph technique will be used to obtain both h&η from a single test as described by Ekkad [11]. Thus, two images with surface temperature distributions are captured at two different times during the transient test.

A net heat flux ratio is used to measure the combined effect of film effectiveness and heat transfer coefficient [12]:

$$\frac{q}{q_o} = \frac{h}{h_o}\left(1 - \frac{\eta}{\emptyset}\right) \quad \dots \quad (7)$$

The value for the overall cooling effectiveness (ø) ranges between 0.5 and 0.7.A typical value is Ø = 0.6, and this in general assumed in the experimental analysis.

The IR images for models surface at each investigated test was captured and stored by thermal camera. These images are transferred to PC. Smart View Software program supplied with Camera can be used to limit the selected area to avoid the effect of the test section walls. The IR images converted to corresponding temperature digital values and then saved as data in Excel sheet.

MATLAB program Software are prepared using a semi-infinite solid assumption presented in chapter three to introduced the film cooling effectiveness and heat transfer coefficient contours.

Equations, (4), (5), (6), and (7) might be solved using MATLAB Software, Smart View Software, and Excel Software. The data were obtained from the selected area denoted by (A_o= 46x135 pixels), in which pixel is the smallest special unit used in a digital picture, this area included sex staggered jet holes as shown in Figure (6).

RESULTS AND DISCUSSIONS

Contours of film cooling effectiveness are calculated from, the test surface temperature distribution, and the measurement of the hot mainstream and coolant air temperatures. Figure (7) show the effect of blowing ratio on detailed film effectiveness distributions for the three cases. From the jet streaks are clearly that the results agree well with results obtained by [6 & 7] where the jet streaks are visible with the highest effectiveness occurring at BR=0.5 near the hole exits for all cases. Also at higher blowing ratios, there is a jet lift-off resulting in lower coverage. However, from the results presented in Figure (7) and as stated by[6&7], the higher blowing ratios show more spreading downstream resulting in higher effectiveness downstream.

Effectiveness contours show clearly that the effectiveness values increases with increase of the blowing ratio and decrease inclination angle. The high effectiveness value may be as a result that the injected cold jet flow close to test surface. The blowing ratio (1.5) case shows more uniform effectiveness contours in the vicinity of the holes than the other cases, and indicated high film cooling effectiveness value.

The local heat transfer coefficients (h) calculated from the data of two IR images taken in success times, ten seconds each capturing image. Figurs (8) present the effect of blowing ratio on (h). This Figure shows that (h) values increases with increased of blowing ratios for all cases. Thus, the mixing between the higher velocity jets and the hot mainstream flow are increasing the local turbulence generation, and this leading to higher heat transfer coefficient.

The span wise average film cooling effectiveness (η_{sa}) are calculated from the local of (η) span wise pixels of each images (46 pixels). Then these values are plotted in x-direction for sixteen stations (16 pixels rows).Figure(9) presents the effect of inclination angles and blowing ratios on span wise averaged film effectiveness. This Figure shows clearly that the highest value of the average effectiveness for (θus =20º, 30º, and 40º) is at hole exit, and then decreased for (θ us = 30º, and 20º) to the lowest value at about X/D = 2, and then increased again due to the flow spreading when X/D exceed 2. While for θ_{us}=40º the lowest values are occurred at about X/D = 3, since the flow of the cold air is flowing close to the test section wall when θus =40º, then increased again for all blowing ratios.

The results of the average film cooling effectiveness (η_o) were obtained at (A_o). The overall averaged film cooling effectiveness was calculated from the values of the local (η) for the pixels in this area, in which this area contains (46 x 135 pixels).Figure (10) shows the effect of blowing ratio on (η_o) for all cases. This Figure shows clearly that for the case (θus = 20º) the values of (η_o) are higher than the other two cases.

The average of the local heat transfer coefficients (h and h_o) were calculated from the experimental data of the parameters (T_w, T_m, T_c, t, k and α) for cooling

cases (h), while the parameters (Tw, Tm, t, k and α) for non- cooling cases (h_o)at the selected area (Ao). Figure (11) shows the effect of blowing ratio on the ratio (h/ho). The highest heat transfer coefficient ratios were obtained at (θus = 20º) and (h/ho) increase with (BR).

In practical application, turbine designers are concerned with the reduction of heat load to the film protected surface. The heat load can be presented by combining film cooling effectiveness (η) and the heat transfer coefficient ratio (h/h_o), therefore the ratio of heat flux (q) with film protected surface to that of the value without film cooling (q_o) can be calculated. These ratios represent the reduction in heat flux at the test surface with presence of coolant air. If the values of these ratios are less than 1, therefore the film coolant is beneficial according to [6], while if the values are greater than 1, therefore the film coolant effects are poor.. Figure (12) presents the effect of blowing ratio on overall heat flux ratios (q/q_o). It is clear from thisFigure that all cases have positive effects of coolant. At blowing ratio 1.5 indicated the best coolant effects than the others. The blowing ratios (2&3) were found not significant.

CONCLUSIONS

The holes distributions and geometry of two rows of staggered holes with opposite orientation angles were taken into account in the investigation at the present work. At the downstream holes row, (θ) is fixed at $0^o$and (θ) at 30°, while at the upstream row,(θ) is fixed at180° and (θus) taken as 40º, 30º, and 20º). These sorts of distributions enhanced the film coolant effectiveness and heat transfer coefficients. For the blowing ratio 0.5 the film cooling effectiveness constricted at the holes exit for all cases, while with the increasing of the blowing ratios up to 1.5, the coolant jets flow were start to spared downstream of the exit holes and gave better film cooling effectiveness. For all cases and blowing ratios the heat flux ratios were found to be less than (1), i. e. good coolant effectiveness is being achievedfor all cases to be studies.

REFERENCES

[1].Han, J.C. and Ekkad, S.V., " Recent Development in Turbine Blade Film Cooling", International Journal of Rotating Machinery, Malaysia, Vol. 7, No. 1, 2001, pp. 21-40.

[2].Han, J.C. and Rallabandi, A. P.,2010, "Turbine Blade Film Cooling Using PSP Technique", Frontiers in Heat and Mass Transfer, Texas, 77843-3123, USA.

[3].Ahn, J., Jung, I.S., and Lee, J.S., "Film cooling from two rows of holes with opposite behavior and adiabatic film cooling effectiveness", International Journal of Heat and Fluid Flow, Vol. 24, 2003, pp. 91-99.

[4].Maiteh, B.Y. and Jubran, B.A., 2004, " Effects of pressure gradient on film cooling effectiveness from two rows of simple and compound angle holes in combination", Energy Conversion and Management, Oman, Vol. 45, PP. 1457-1469.

[5].Dhungel, A.,Phillips,A., Ekkad, S.V., and Heidmann, J.D., 2007, "Experimental Investigation of a Novel Anti-Vortex Film Cooling Hole Design", ASME IGTI Turbo Expo, Montreal, Paper GT 2007-27419.

[6]. Dhungel,Lu, Y., A.,Ekkad, S.V., and Bunker, R.S., 2007, "Effect of Trench Width and Depth on Film Cooling from Cylindrical Holes Embedded in Trenches", ASME Paper GT 2007-27388.
[7]. Dhungel, Lu, Y., A., Ekkad, S.V., and Bunker, R.S., 2007, "Film Cooling Measurements for Cratered Cylindrical Inclined Holes", ASME Paper GT 2007-27386.
[8].Dia, P. and Lin, F., 2011, "Numerical study on film cooling effectiveness from shaped and crescent holes", Heat Mass Transfer, Vol. 47, PP. 147-154.
[9].Lee, K.D. and Kim, K.Y., 2011,"Surrogate based optimization of a laidback fan-shaped hole for film-cooling", International Journal of Heat and Mass Transfer, Republic of Korea, Vol. 32, PP. 226-238.
[10].Holman, J.P. and Bhattacharyya, S., "Heat Transfer", Ninth Edition, New Delhi, McGraw-Hill, 2008.
[11].Ekkad, S.V., Ou, S., and Rivir, R.V., "A Transient Infrared Thermography Method for Simultaneous Film Cooling Effectiveness and Heat Transfer Coefficient Measurements from a single test", GT 2004-54236, Proceedings of ASME Turbo Expo 2004, Vienna, Austria.
[12].Ekkad, S.V., and Zapata, D., "Heat transfer coefficients Over a Flat Surface with Air and CO2 Injection Through Compound Angle Holes Using a Transient Liquid Crystal Image Method", ASME Journal of Turbomachinery Vol. 119, No. 3, 1997, pp. 580-586.

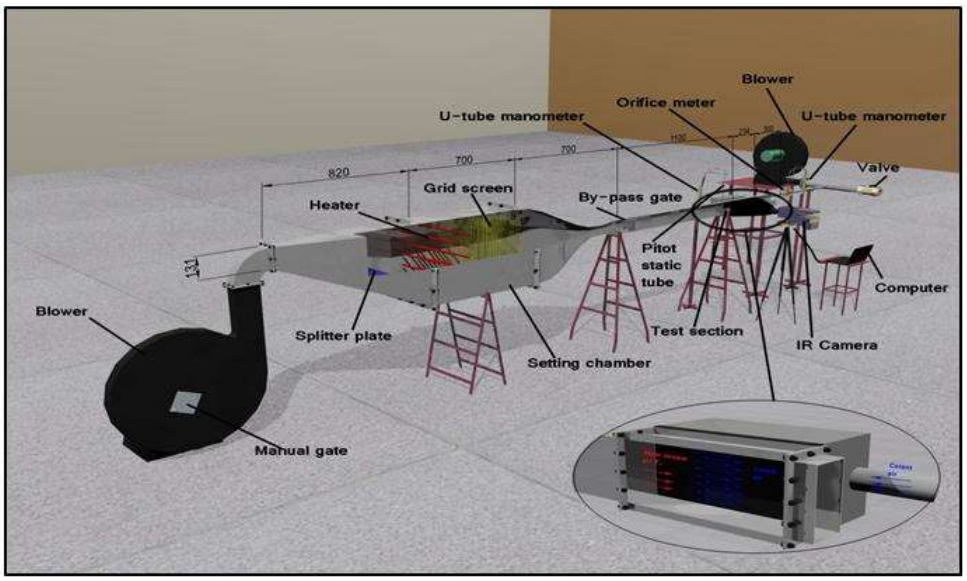

Figure (1) Schematic of the test rig.

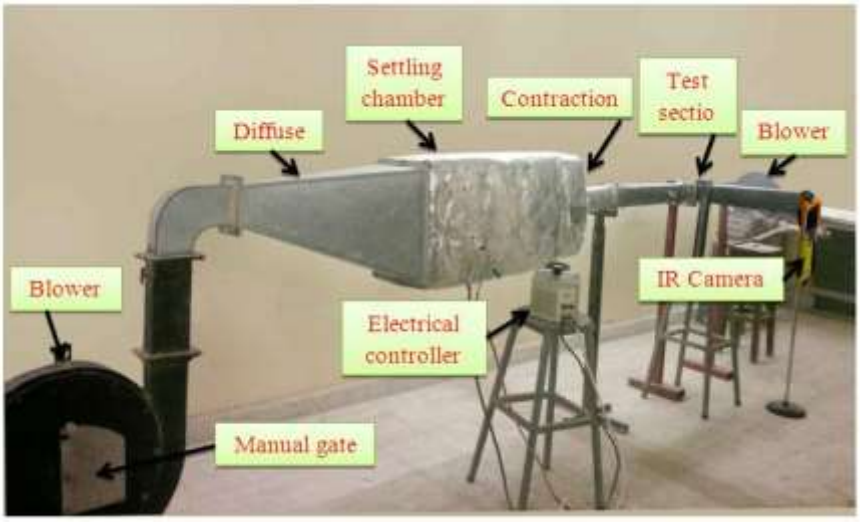

Figure (2)Photograph of the test rig.

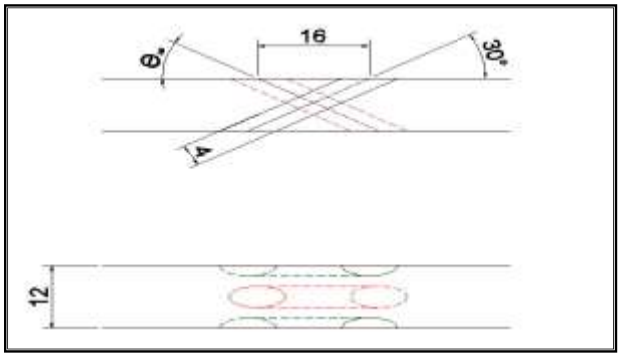

Figure (3) holes rows arrangement of hole rows.

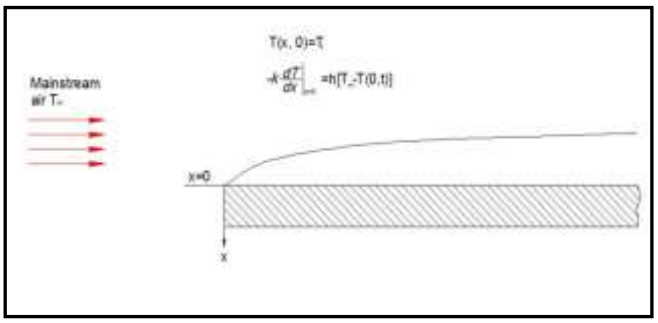

Figure (4) Flow over a flat plate.

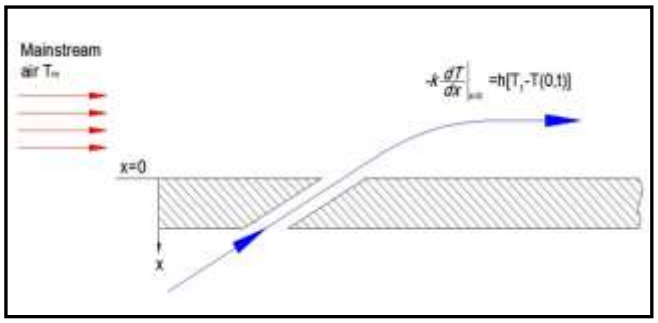

Figure (5) Film cooling over a flat plate.

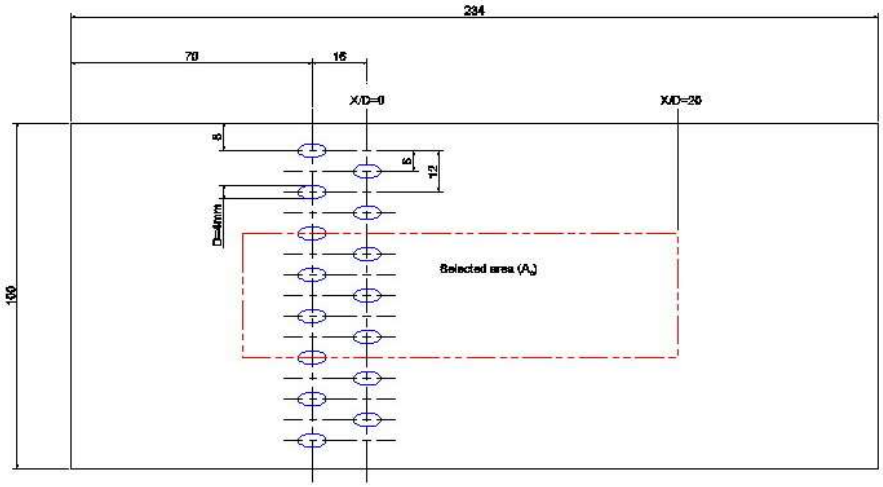

Figure (6) the middleselected area of the test section (A_o).

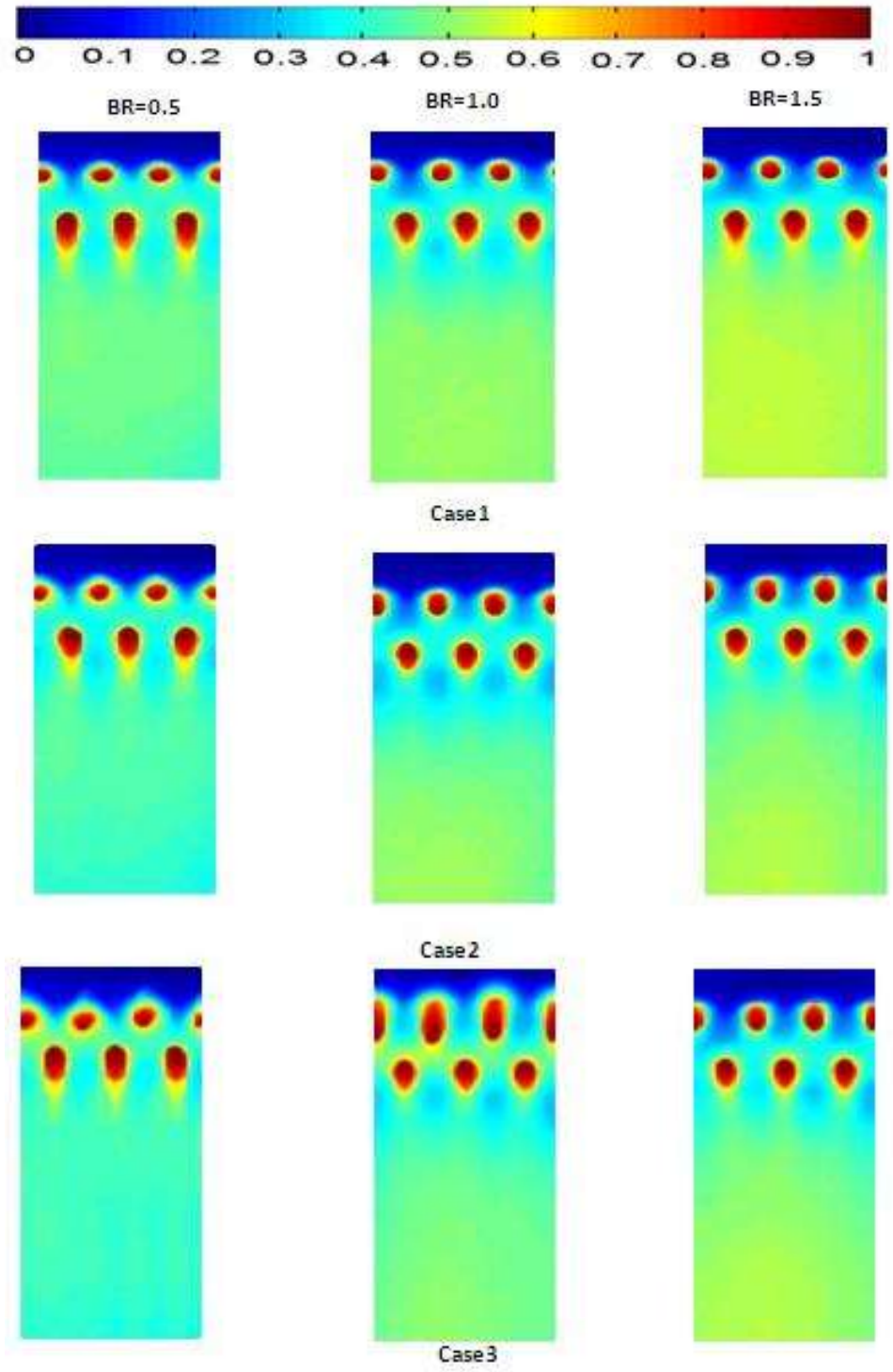

Figure (7) contours of local film cooling effectiveness for cases 1,2, and 3 at different blowing ratio.

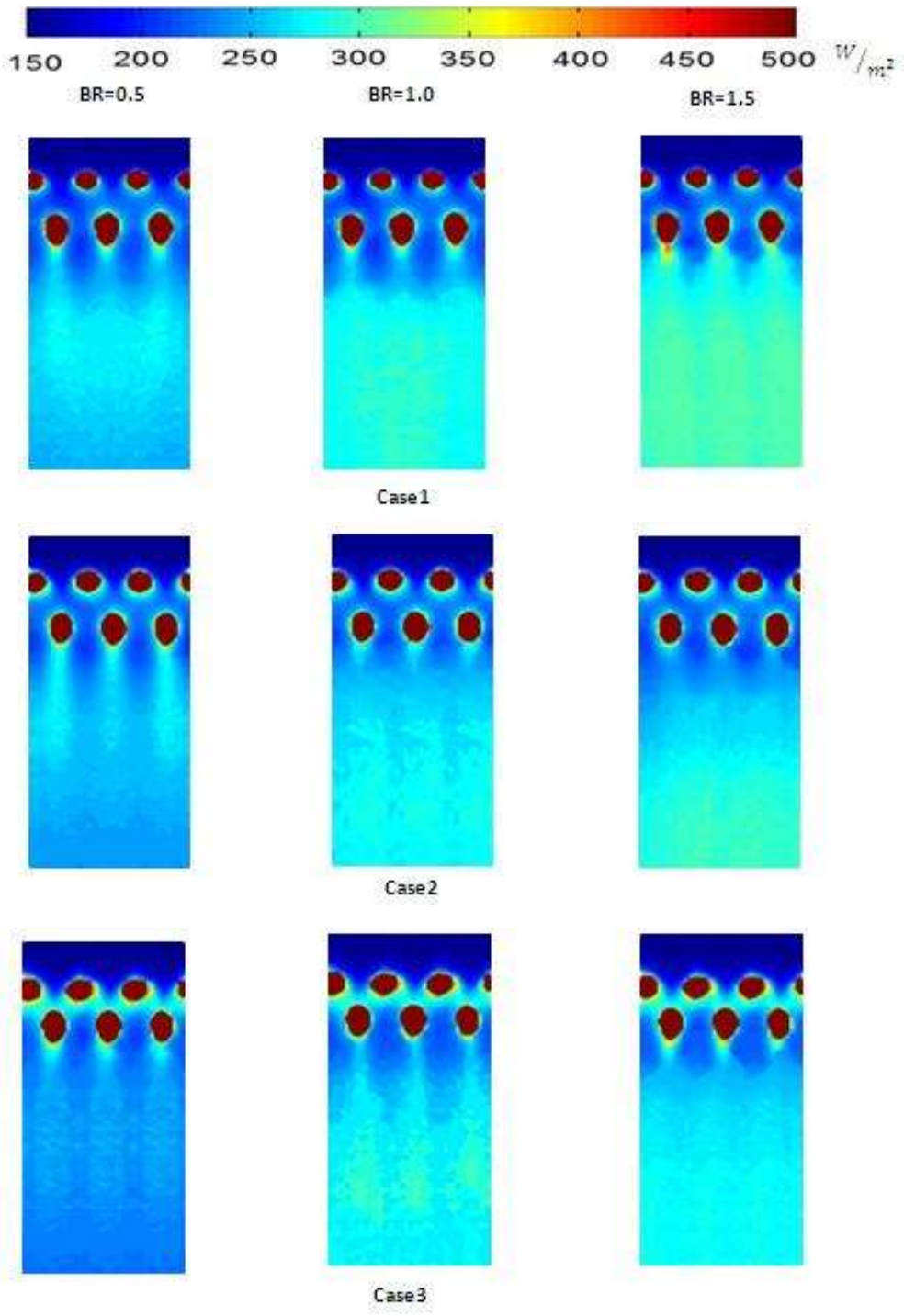

Figure (8) contours of local heat transfer coefficient for cases 1,2, and 3 at different blowing ratio.

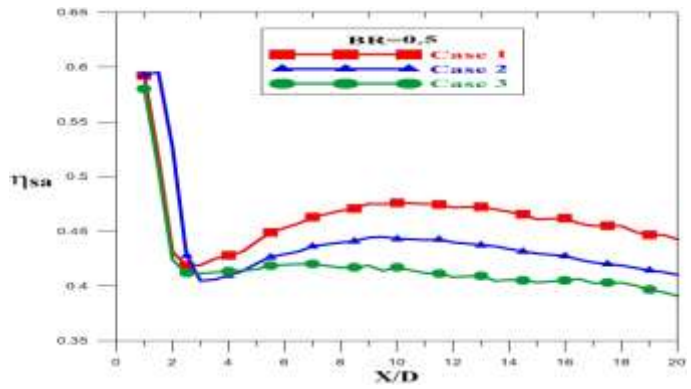

(a)

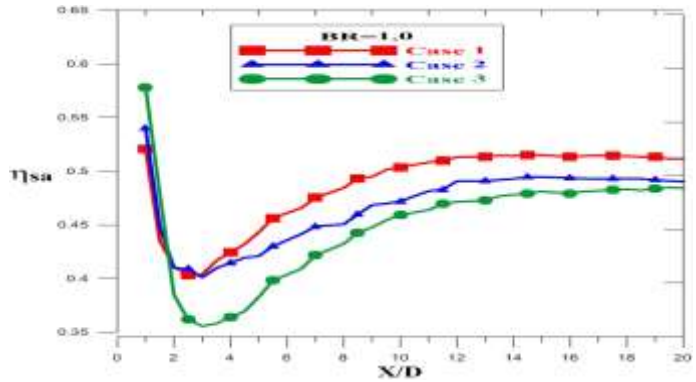

(b)

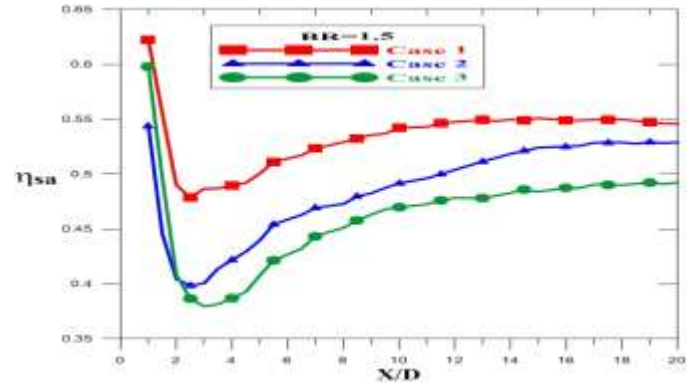

(c)

Figure (9) Effect of Cases on Spanwise Averaged Film Cooling Effectiveness Distributions at: (a) BR=0.5, (b) BR=1.0 and (c) BR=1.5.

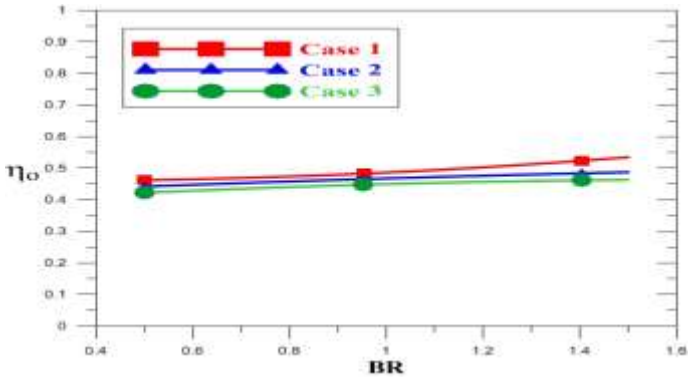

Figure (10) Effect of Blowing Ratio on Area-Averaged film cooling effectiveness.

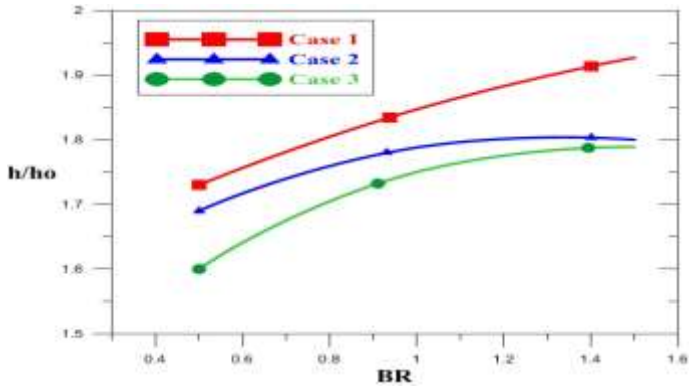

Figure (11) Effect of Blowing Ratio on Overall Area-Averaged Heat Transfer Coefficient Ratio.

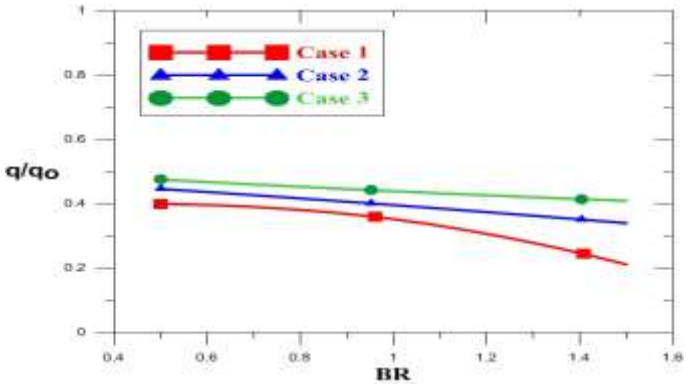

Figure (12) Effect of Blowing Ratio on Overall Heat Flux Ratio.